

Research Article

Abnormal Expression of Connexin43 in Cardiac Injury Induced by S-Band and X-Band Microwave Exposure in Rats

Yue Yin , Xinping Xu, Yabing Gao, Juan Wang, Binwei Yao, Li Zhao, Haoyu Wang, Hui Wang, Ji Dong, Jing Zhang , and Ruiyun Peng 

Beijing Institute of Radiation Medicine, Beijing 100850, China

Correspondence should be addressed to Jing Zhang; zhang115614@163.com and Ruiyun Peng; pengry@bmi.ac.cn

Received 27 August 2021; Accepted 6 November 2021; Published 17 December 2021

Academic Editor: Herney A. Garcia-Perdomo

Copyright © 2021 Yue Yin et al. This is an open access article distributed under the Creative Commons Attribution License, which permits unrestricted use, distribution, and reproduction in any medium, provided the original work is properly cited.

Although the effects of microwave exposure on the heart have gradually become the focus of domestic and foreign scholars, the biological effects caused by different doses and different frequency bands of exposure are still unclear. In this study, we will investigate the damaging effect of S-band and X-band microwave composite exposure on cardiac structure and function, as well as the pathophysiological significance of Cx43 in cardiac conduction dysfunction after exposure. We used S- and X-band radiation sources with the average power density of 5 and 10 mW/cm² to expose Wistar rats to single or composite exposure. At the 6th hour, on the 7th, 14th, and 28th days after exposure, ECG was used to detect the electrical conduction of the heart, and the myocardial enzyme was measured by the automatic biochemical analyzer. We selected the observation time points and groups with severe damage to observe the changes of myocardial structure and ultrastructure with an optical microscope and TEM; and to detect the expression and distribution of Cx43 by western blotting and immunohistochemistry. After exposure, the heart rate increased, the P wave amplitude decreased, and the R wave amplitude increased; the content of the myocardial enzyme in serum increased; the structure and ultrastructure of cardiac tissue were damaged. The damage was dose-dependent and frequency-dependent. The expression of Cx43 in myocardial tissue decreased, and distribution was abnormal. Taken together, these findings suggested that the mechanism of abnormal electrical conduction in the heart of rats by S- and X-band microwave exposure might be related to the decreased expression and disordered distribution of Cx43 after microwave exposure.

1. Introduction

The influence of electromagnetic fields, especially microwave radiation, on biological systems has attracted much interest for a long time [1, 2]. Microwave radiation may cause different biological effects on the cardiovascular system [3, 4]. Xu et al. [5] have found that after 11 mW/cm² microwave radiation in rhesus monkeys, arrhythmia occurred. ECG results indicated the decrease of the R-H value and T wave peak, and some animals had wide QRS waves, which suggested the damaged heart conduction tissues and myocardial fibers. Zhang et al. [6] observed that after long-term microwave radiation with average power densities of 0, 2.5, 5, and 10 mW/cm² in rats. The myocardial enzymes activities and ion concentrations were imbalanced, which indicated micro-

wave radiation could cause damage to rats' myocardia. Another study used radiofrequency electromagnetic radiation with a frequency of 1800 MHz to continuously radiate rats for 5 weeks. They found irregular myocardial fibers and widened fiber gaps, which might cause abnormal contraction of myocardia [7].

Cx43, a member of the gap junction protein family, is widely distributed in the cardiovascular system [8], nervous system [9], immune system [10], and tumor tissues [11], participating in normal cell-to-cell communication and mediating tumor immune response. It is the most widely distributed and most abundant protein in cardiomyocytes [12]. Cx43 plays a decisive role in the electrical conduction of the heart coexpressed with ion channels [13, 14] and leads to an increased susceptibility to arrhythmias by dephosphorylation [15].

Although a previous study addressed that the S- and X-band microwave radiation could damage the structure and the function of the heart [16], there has been no research showing the effect of S- and X-band microwave composite exposure on cardiac injury. And the relationship between heart injury and Cx43 after microwave exposure has not been reported yet. In this study, we analyzed the changes in the structure and function as well as the changes in Cx43 expression and distribution of the heart after composite exposure. Furthermore, we explored the pathophysiological significance of Cx43 in cardiac electrical conduction abnormalities after composite exposure in rats. Our research would provide novel approaches to injury mechanisms and the necessary basis of protective targets.

2. Materials and Methods

2.1. Animals and Experimental Approval. 140 secondary male Wistar rats (200 ± 20 g) were purchased from Beijing Weitonglihua Experimental Animal Center. Rats were fed in an SPF-grade animal facility with the standard laboratory conditions ($22 \pm 1^\circ\text{C}$, 60% feeding density, 12 hours circadian rhythm, and 5 rats per cage), eating and drinking freely. All protocols were approved by the Beijing Institute of Radiation Medicine Animal Care and Use Committee. The experiments were approved by the Ethical Committee of the Academy of Military Medical Sciences, and the authorization number was IACUC-DWZX-2021-650.

2.2. Groups and Microwave Exposure. In this experiment, “S” and “X” represented the 2.856 GHz and 9.375 GHz microwave exposure groups. To eliminate the influence of rats’ weight in the experiment, 140 rats were divided into 7 groups equally by the stratified random method. The group assignment was as follows: control group (C group), 5 mW/cm² S-band exposure group (S5 group), 10 mW/cm² S-band exposure group (S10 group), 5 mW/cm² X-band exposure group (X5 group), 10 mW/cm² X-band exposure group (X10 group), 5 mW/cm² composite exposure group (SX5 group), and 10 mW/cm² composite exposure group (SX10 group).

Rats were fixed in the radiation box made of plexiglass, and the rats were exposed to the radiation source with the exposure table rotated to eliminate positional influence. Rats in the single-band exposure groups were radiated for 6 min, and those in the composite-band exposure groups were radiated by each band for 6 min. During the exposure period, rats in the C group were also handled parallel to those in the exposure groups, except for microwave radiation. Before and immediately after microwave exposure, 10 rats were selected randomly from each group, and detected the core temperature by the portable thermometer JM222 (Beijing Zhongwang, China).

2.3. ECG Examination. At the 6th hour and on the 7th, 14th, and 28th days after exposure, the multichannel physiological recording and analysis system (BIOPAC, USA) was used to detect the rats’ ECG. There were 5 rats in each group. And the rats were weighed and injected intraperitoneally with

1% pentobarbital sodium (1 mL/100 g). After anesthesia, the operation process was as follows: shaving the rats’ limbs, fixing them in the supine position, and disinfecting with 75% ethyl alcohol. The electrode wires included red (right upper limb), black (right lower limb), and green (left lower limb). The electrode needles were, respectively, pierced into the subcutaneous of their corresponding limbs, connected to the ECG bioamplifier with a sensitivity of 2000 Hz. The rats were in a quiet state and recorded continuously for 3 min. Then we analyzed and calculated changes in indicators such as the heart rate, P wave, and R wave.

2.4. Serum Biochemical Analysis. At the 6th hour and on the 7th, 14th, and 28th days after exposure, 5 rats in each group were taken. After the rats were anesthetized (the specific operation is the same as method 3), 3 mL of blood was collected from the inferior vena cava to prepare serum. An automatic biochemical analyzer (Coulter JTIR, USA) was used to determine the activities of AST, CK, and LDH.

2.5. Structure of Rats’ Myocardial Tissue. On the 7th day after exposure, the rats were anesthetized and the hearts were removed, with 5 rats in each group. Removed hearts were fixed in 10% formalin fixative for 1 week. After dehydration, transparency, and dipping in wax, the paraffin-embedded heart tissues were cut into slices of 5 μm . After dried at 60°C for 2 days and deparaffinized, the tissues were stained by H&E. The stained slices were observed and photographed by the optical microscope (Leica, Germany).

2.6. Ultrastructure of Rats’ Myocardial Tissue. On the 7th day after exposure, the rats were anesthetized and the hearts were removed, with 3 rats in each group. A fresh tissue block of about 1 mm³ was taken from the apex of the heart and placed into 2.5% glutaraldehyde fixative for 2 h. Next, the tissue pieces were fixed in 1% osmic acid for 1 h. After dehydration with gradient ethanol, acetone transition, and embedded in Epon 812 resin, the tissues were cut into semithin sections to locate where the damage was the most severe. Then, the semithin slices were made into 70 nm ultrathin sections and stained with lead-uranium. At last, the slices were observed and photographed by a TEM (Hitachi, Japan).

2.7. Expression of Cx43 in Rats’ Myocardia. On the 7th day after exposure, the total protein of myocardial tissues of rats was extracted and subjected to western blotting in groups C, S10, X10, and SX10. The operation steps were as follows: cut out 20 mg of each frozen heart kept in the refrigerator, added 4°C precooled PBS, washed the blood, and discarded the liquid; added 200 μL tissue lysate solution at the ratio of 1 mg/10 μL (lysate : protease inhibitor = 100 : 1) and cut the tissue into pieces; 3000 r/s homogenized for 4 times, 15 s each time by an automatic homogenizer, bathed in ice for 10 min, centrifuged 12000 r/min, for 15 min at 4°C, and collected the supernatant; and determined the protein concentration by the BCA protein concentration determination kit (Thermo, USA). The protein was mixed with the loading buffer (4:1), denatured in boiled water bath for 10 min, and added the cooled sample on the SDS-PAGE. After the steps of

electrophoresis, membrane transfer, and blocking, the rabbit anti-Cx43 (TBST diluted 1:1000; Abcam, USA) and mouse anti-GAPDH (TBST diluted 1:10000; Abcam, USA) were added, shook slowly overnight at 4°C in a shaker, and washed with TBST for 3 × 10 min; the HRP-labeled goat anti-rabbit IgG (TBST dilution 1:10000; Beyotime, China) and goat anti-mouse IgG (TBST solution dilution 1:10000; Beyotime, China) were added, shook for 1 h at room temperature, and washed with TBST for 3 × 10 min; the clear bands were semiquantified the optical density value and performed statistical analysis.

2.8. Distribution of Cx43 in Rats' Myocardia. On the 7th day after exposure, the hearts of 5 rats in groups C, S10, X10, and SX10 were fixed in 10% formalin fixative solution for 1 week, and after dehydration, transparency, wax immersion, paraffin embedding, and 5 μm film production, the immunohistochemical experiment was carried out. The main steps were as follows: deparaffinized to water; put the tissue section into the boiling citrate buffer, continuously heated in a microwave oven for 10-15 min, and cooled to room temperature naturally; added the endogenous peroxidase blocker dropwise and incubated in the dark for 10 min at room temperature; added rabbit anti-Cx43 (diluted in PBS, 1:1000; Abcam, USA) and incubated at 37°C for 1 h; added reaction enhancement solution dropwise and incubated at room temperature for 20 min; dropped HRP-labeled goat anti-rabbit IgG and incubated at 37°C for 30 min; added DAB and observed under the microscope to control the color development time; used hematoxylin counterstain; and dehydrated transparent mount and observed and took pictures under the optical microscope. PBS was used to wash for 3 × 5 min between every two steps.

2.9. Statistical Analysis. Data in the article were expressed in terms of mean ± SD, and the SPSS19.0 version was used for statistical analysis. One-way ANOVA and independent sample *t*-tests were applied to statistics analysis.

The acceptable significance level for all tests was $P < 0.05$. According to the comparison objective and meaning, the significant signs were classified as follows: significant exposure effect, * $P < 0.05$ and ** $P < 0.01$ (comparison between the radiation group and the C group); significant frequency-dependent effect, $^{\wedge}P < 0.05$ and $^{\wedge\wedge}P < 0.01$ (X10 and S10, X5 and S5); significant dose-dependent effect, $^{\#}P < 0.05$ and $^{\#\#}P < 0.01$ (S10 and S5, X10 and X5); and significant composite exposure effect, $^{\wedge}P < 0.05$ and $^{\wedge\wedge}P < 0.01$ (SX10 and S10, SX5 and S5) and $^{\wedge}P < 0.05$ and $^{\wedge\wedge}P < 0.01$ (SX10 and X10, SX5 and X5).

3. Results

3.1. Microwave Radiation Induced Abnormal ECG Results. The heart rate, P waves, and R waves of rats were measured at the 6th hour, on the 7th, 14th, and 28th days after exposure ($n = 5$):

- (1) At the 6th hour after exposure, compared with group C, the heart rate of rats increased in the radiation

groups ($P < 0.01$ or 0.05). On the 7th day after exposure, the heart rate still increased in the S5, X10, SX5, and SX10 groups ($P < 0.05$) (Figure 1)

- (2) At the 6th hour after exposure, compared with group C, the P wave amplitude of the S10 and SX5 groups decreased ($P < 0.05$); the frequency-dependent effect results showed that the S10 group decreased more significantly than the X10 group ($P < 0.05$); the dose-dependent effect results stated that the S10 group decreased more significantly than the S5 group ($P < 0.05$). On the 7th day after exposure, the comparison with group C suggested that the P wave amplitude of the S10 and X5 groups decreased ($P < 0.05$) (Figure 2)
- (3) At the 6th hour after exposure, compared with group C, the R wave amplitude increased in the X5 and SX5 groups ($P < 0.01$ or 0.05). On the 7th day after exposure, the R wave amplitude of the S5, X5, and X10 groups increased ($P < 0.01$ or 0.05) (Figure 3)

3.2. Microwave Radiation Increased Myocardial Enzyme Activity. The activities of AST, CK, and LDH (U/L) were detected in the serum of rats at the 6th hour, on the 7th, 14th, and 28th days after exposure ($n = 5$):

- (1) At the 6th hour after exposure, compared with group C, the activity of AST increased significantly in the S10, SX10, and X10 groups ($P < 0.01$ or 0.05). On the 7th day after exposure, compared with group C, the activity of AST significantly increased in the S10 and SX10 groups ($P < 0.01$); and the dose-dependent effect results showed that the S10 group increased more significantly than the S5 group ($P < 0.05$), and the SX10 group increased more significantly than the SX5 group ($P < 0.01$); and the frequency-dependent effect results showed that the S10 group increased more significantly than the X10 group ($P < 0.01$) (Figure 4(a))
- (2) At the 6th hour after exposure, compared with group C, the activity of CK increased in the S10, SX5, SX10, and X10 groups ($P < 0.01$ or 0.05); and on the 7th day after exposure, the SX10 group increased ($P < 0.05$) (Figure 4(b))
- (3) At the 6th hour after exposure, compared with group C, the activity of LDH increased significantly in the S10, X5, and SX10 groups ($P < 0.01$); and on the 7th day after exposure, the S10, X10, and SX10 groups increased significantly ($P < 0.01$); on the 14th day after exposure, the S10, X10, and SX10 groups increased ($P < 0.05$) (Figure 4(c))

3.3. Microwave Radiation Caused Abnormal Myocardial Structure. Based on the previous experiment results, at the 6th hour and on the 7th day after exposure, rats received heavier damage than at other time nodes. Therefore, this experiment selected the 7th day with heavier damage as the time point of tissue structure observation.

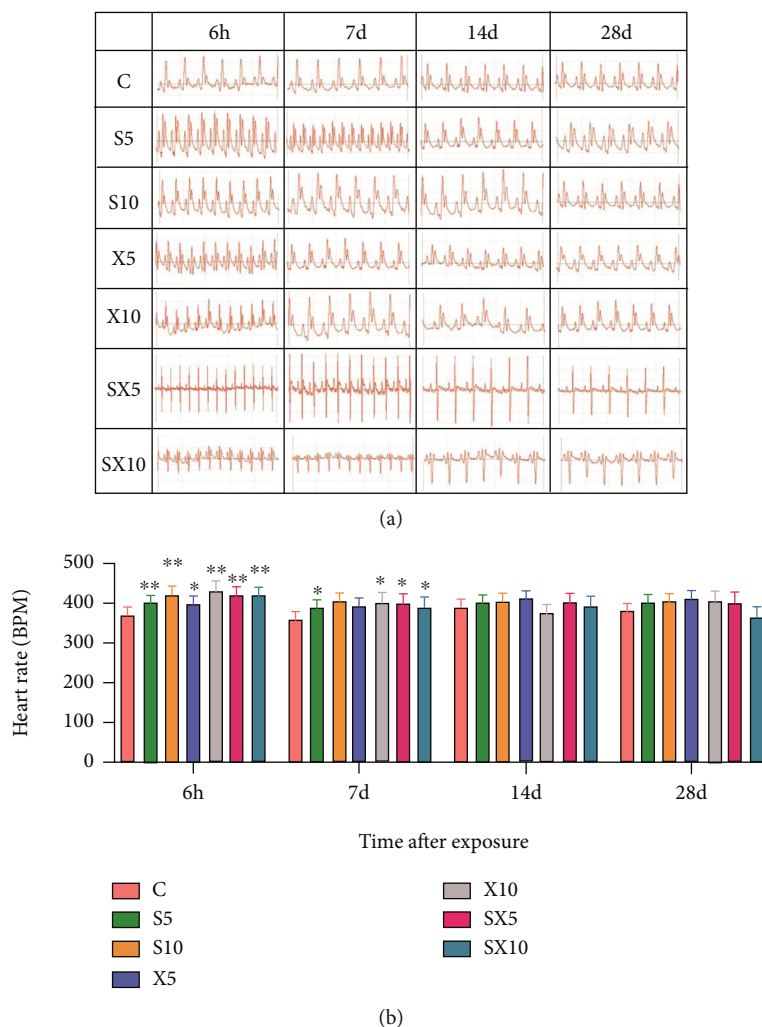


FIGURE 1: Heart rate of ECG of rats after S- and X-band microwave exposure. (a) ECG records. (b) Analysis of the heart rate. Data was expressed as means \pm SD. Compared with the C group, * meant $P < 0.05$ and ** meant $P < 0.01$ ($n = 5$).

On the 7th day after exposure, the myocardial fibers were neatly arranged, and nuclei of endothelial cells were fusiform, and myocardial cells were oval in the C group. In the S5, X5, and X10 groups, there was no significant change in the myocardial tissue structure. In the S10, SX5, and SX10 groups, the myocardial fiber arrangement of rats was disordered and wavy, and nuclear pyknosis was occasionally seen. The above injuries had a dose-dependent effect. The arrangement of myocardial fibers was disordered, and the structure changes after exposure, which suggested that it might be related to impaired heart function (Figure 5).

3.4. Microwave Radiation Caused Abnormal Myocardial Ultrastructure. Based on the results of cardiac function testing, this experiment chose the 7th day with heavier damage as the time node for tissue ultrastructure observation. On the 7th day after exposure, under the electron microscope, myocardial fibers in group C were arranged neatly, mitochondrial cristae were clear and complete, and the intercalated disk structure was continuous and folded. There was no obvious abnormality in the ultrastructure of the S5 and

X5 groups, and the myocardial fibers were arranged neatly, and the mitochondrial structure was relatively complete. Mitochondrial cavitation occurred in the S10, X10, SX5, and SX10 groups, intercalary disk structure was broken and incomplete, and changes in the arrangement of myocardial fibers were disordered. Mitochondrial structure damage after exposure indicated abnormal energy metabolism. Intercalated disk structure changes might cause damage to cell connection structure, so that chemical coupling and electrical coupling between cells are affected (Figure 6).

3.5. Microwave Radiation Decreased the Expression of Cx43 in Myocardia. From the above experimental results, it was found that the 10 mW/cm² single and composite exposure groups suffered significant damage on the 7th day after exposure. The 7th day was selected as the observation time point to detect the Cx43 content in the myocardial tissues of the C, S10, X10, and SX10 groups. The total protein was extracted from myocardial tissues and western blot experiments were performed to semiquantify the content of Cx43. The results showed that on the 7th day after exposure, the content of

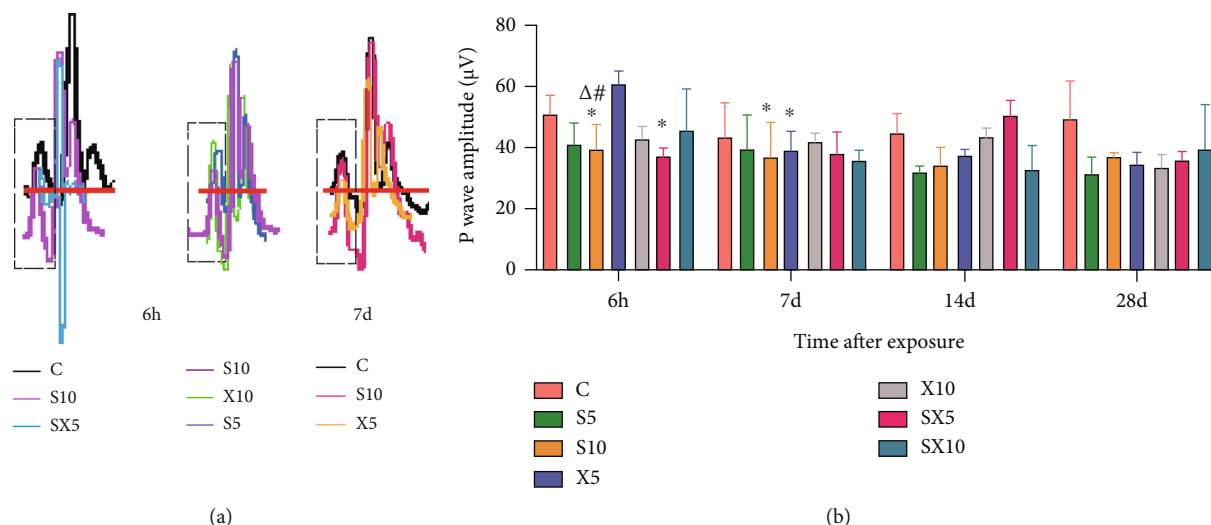


FIGURE 2: P wave of ECG of rats after S- and X-band microwave exposure. (a) Changes of the P wave (the dotted line boxes show the P wave). (b) Analysis of the P wave amplitude. Data was expressed as means \pm SD. Compared with the C group, * meant $P < 0.05$ and ** meant $P < 0.01$; for significant frequency-dependent effect, Δ meant $P < 0.05$; for significant dose-dependent effect, # meant $P < 0.05$ ($n = 5$).

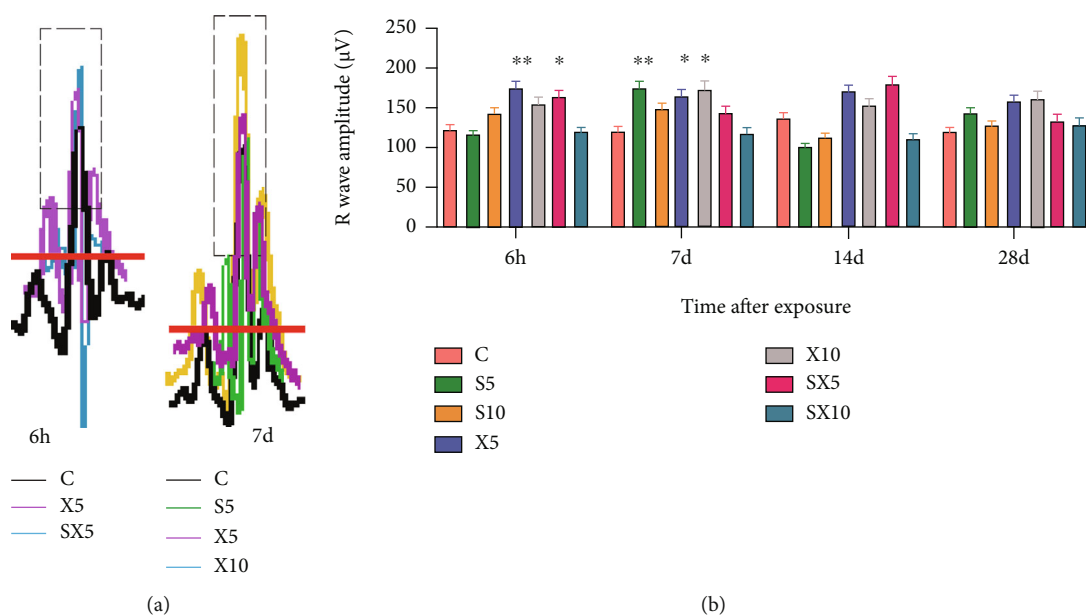


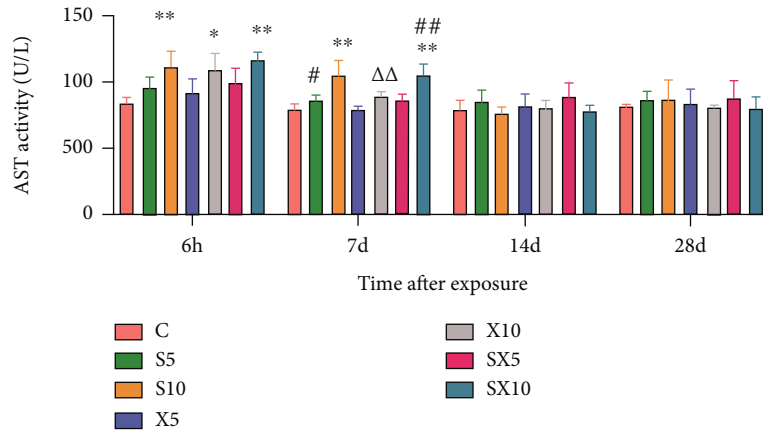
FIGURE 3: R wave of ECG of rats after S- and X-band microwave exposure. (a) Changes of the R wave (the dotted line boxes show the R wave). (b) Analysis of the R wave amplitude. Data was expressed as means \pm SD. Compared with the C group, * meant $P < 0.05$ and ** meant $P < 0.01$ ($n = 5$).

Cx43 in the SX10 group was significantly reduced compared with that in the C group ($P < 0.01$), and the content in the S10 and X10 groups was reduced ($P < 0.05$). Based on the important regulatory role of Cx43 in cardiac electrical conduction, the decrease of Cx43 suggested that it might be related to cardiac electrical conduction disorders (Figure 7).

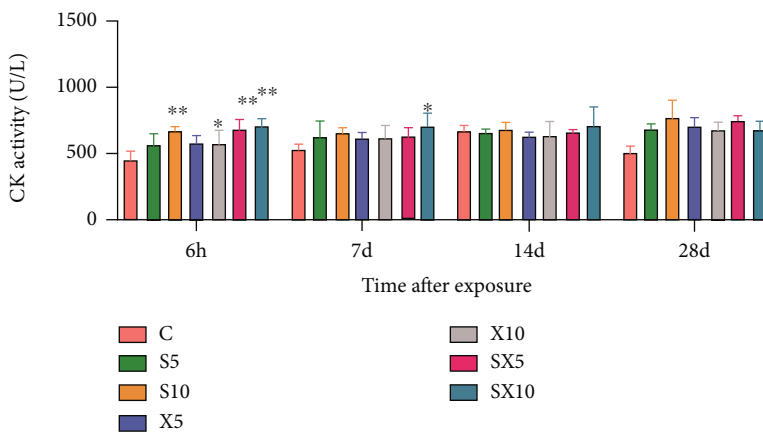
3.6. Microwave Radiation Induced the Abnormal Distribution of Cx43 in Myocardia. At present, there is no reliable quantitative method for the positive signal of Cx43 immunohistochemistry, so only the optical microscope

observation has been used for preliminary exploration in this experiment.

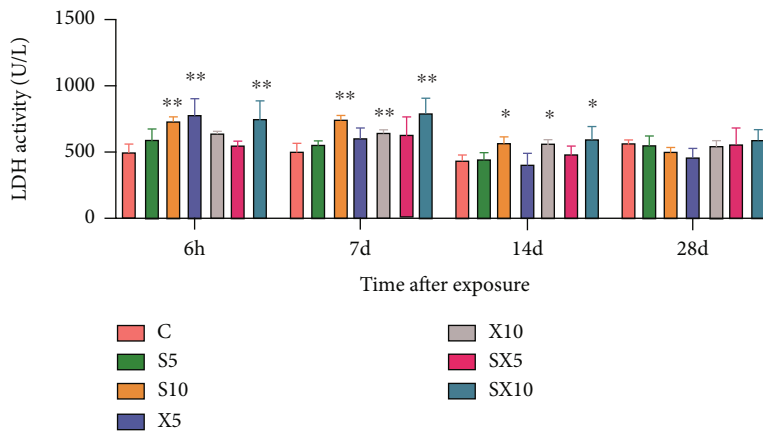
The myocardial tissues of rats in the C, S10, X10, and SX10 groups were selected for immunohistochemical experiments on the 7th day after exposure. The results suggested that Cx43 in group C was distributed at the end-to-end junction of the two cells [17], in a strip shape, perpendicular to the long axis of the cardiomyocytes. Compared with the C group, the Cx43 distribution in the SX10 group was the most disordered, and the positive signal at the end-to-end junction was significantly reduced and scattered. S10 and X10



(a)



(b)



(c)

FIGURE 4: Changes of myocardial enzyme activity of rats after S- and X-band microwave exposure. (a) AST activity. (b) CK activity. (c) LDH activity. Data was expressed as means \pm SD. Compared with the C group, * meant $P < 0.05$ and ** meant $P < 0.01$; for significant frequency-dependent effect, $\Delta\Delta$ meant $P < 0.01$; for significant dose-dependent effect, ## meant $P < 0.01$ ($n = 5$).

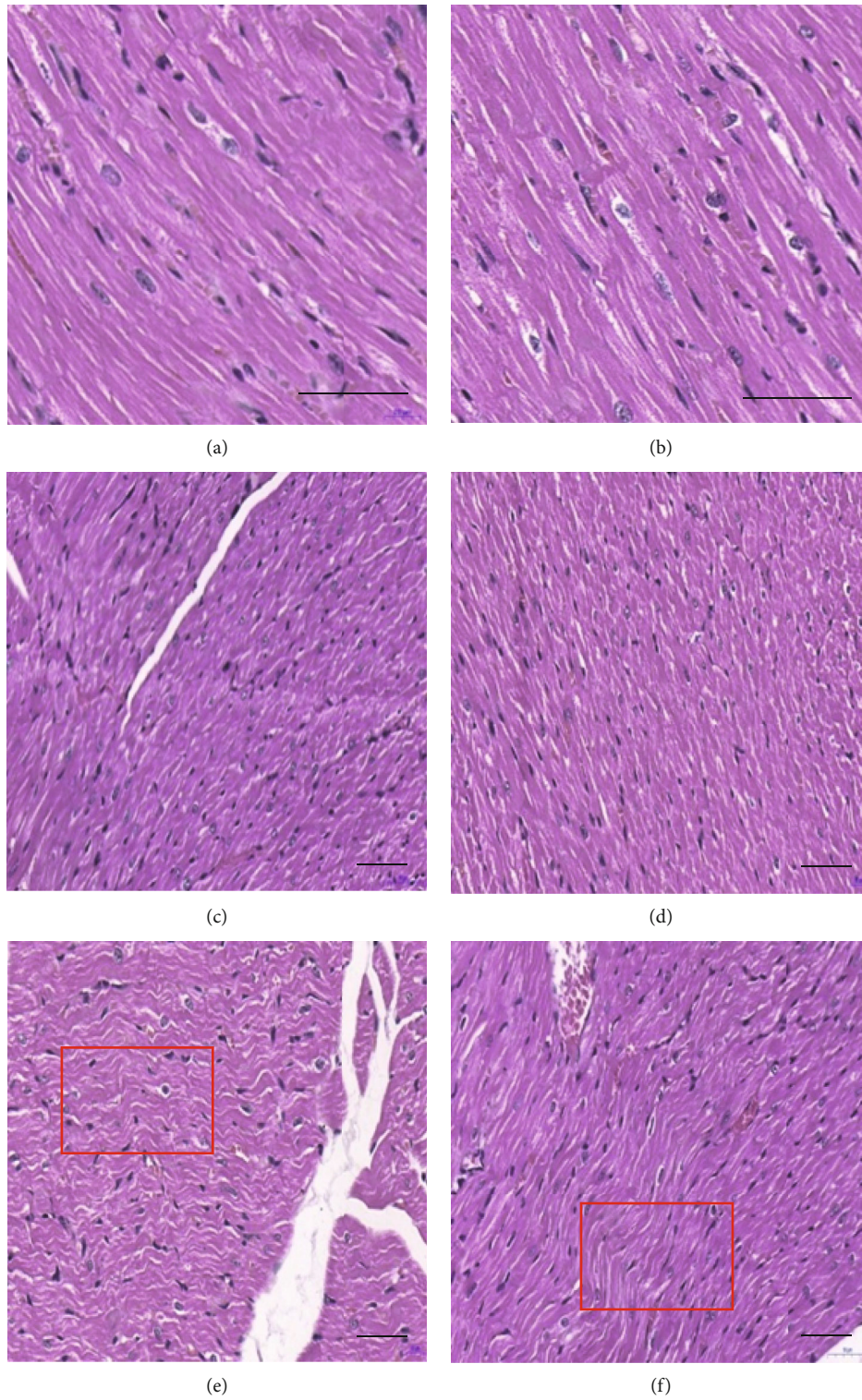
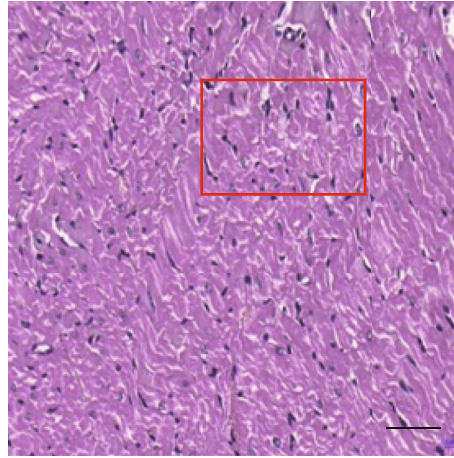


FIGURE 5: Continued.



(g)

FIGURE 5: Changes of myocardial structure of rats on the 7th day after S- and X-band microwave exposure. (a) C group. (b) S5 group. (c) S10 group. (d) X5 group. (e) X10 group. (f) SX5 group. (g) SX10 group. (a, b) $\times 400$. (c–g) $\times 200$. Scale bar = 50 μm . The red frame indicated wavy fibers.

groups were reduced, but there was no significant difference between the groups. The distribution of Cx43 and the decrease of the positive signal after exposure might relate to cardiac electrical conduction disorder, which was consistent with the results of the western blot experiment (Figure 8).

4. Discussion

The heart is one of the target organs that are relatively sensitive to microwave radiation. Previous studies have shown that microwave radiation affected both the function and the structure of the heart. However, the effect of S- and X-band microwave composite radiation on heart damage has not been reported yet.

In the ECG waveform, the P wave is the depolarization wave of the left and right atria, and the QRS wave is the depolarization wave of the left and right ventricles [18]. Through the analysis of the waveform, we could judge the changes of depolarization potential and time in various parts of the heart, which would be helpful to diagnose and prevent arrhythmia in time. In this study, the changes of cardiac function in rats after microwave exposure were indicated by analyzing the results of ECG, and the damage of cardiac conduction function in rats at the 6th hour and on the 7th day after microwave exposure was confirmed, which showed that the heart rate increased, the P wave amplitude decreased, and the R wave amplitude increased. The results might be related to the changes of depolarization potential and depolarization time of atria and ventricles.

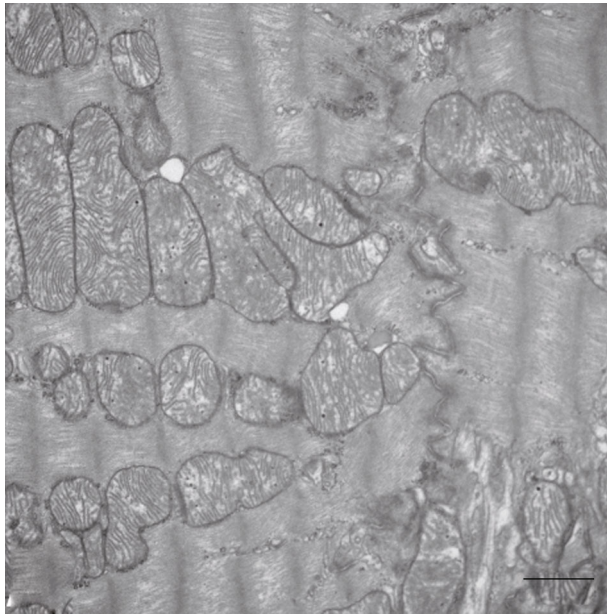
Myocardial enzymes are specific enzymes found in cardiomyocytes, including AST, CK, and LDH. When myocardial cells were damaged, myocardial enzymes would increase at a certain time, which could be combined with ECG or other relevant tests to determine the extent and type of damage [19]. In this study, the changes of cardiac function in rats after microwave exposure were detected by serum biochemical analysis.

The results showed that the heart was damaged at the 6th hour and on the 7th day after exposure, and the activities of AST, LDH, and CK were increased. Those results mentioned above might be related to the damage of cell membrane structure and the change of permeability, which might lead to the myocardial enzyme entering the blood.

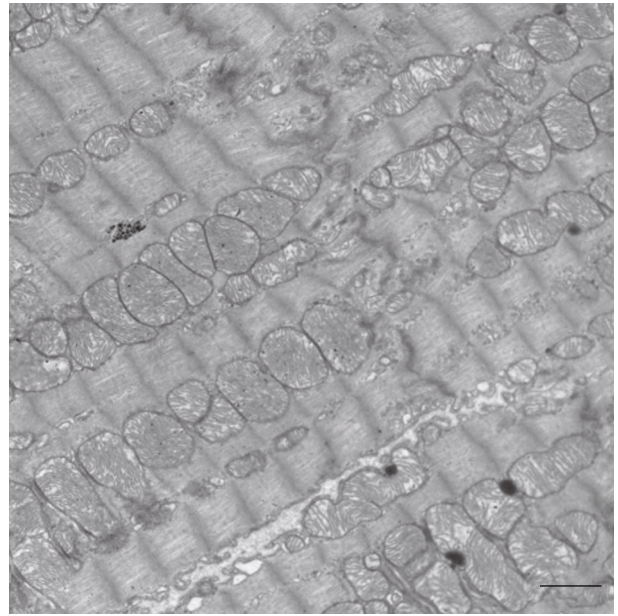
In this study, the changes in the structure and ultrastructure of the rats' heart after microwave radiation were detected by the methods of optical microscope observation after H&E staining and TEM observation. It was clear that the heart structure was damaged at the 6th hour and on the 7th day after exposure, and the damage was more serious on the 7th day. After the 7th day, a recovery trend presented. Under the optical microscope, the main manifestations of the damage showed that the myocardial structure was disordered and wavy. Under the TEM, the myocardial fiber was disordered, the mitochondria was cavitated, and the intercalary disk structure was incomplete.

These results suggested that the S- and X-band microwave radiation could cause damage to the structure and function of the rat hearts. The functional damage was severe at the 6th hour and on the 7th day, and the structural damage appeared on the 7th day. However, 7 days later, both structural damage and functional damage were recovered. The dose- and frequency-dependent effects were consistent with the results of previous studies.

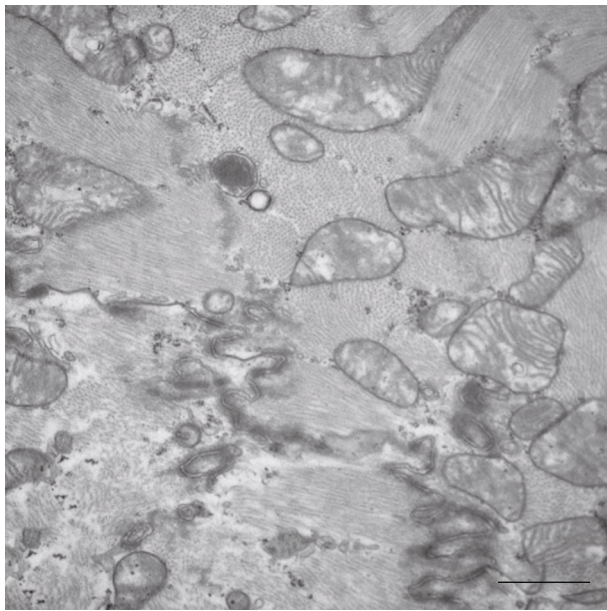
Cx43 is the most abundant gap junction protein in the heart and plays an important role in cardiac electrical conduction. Changes in its expression, distribution, and dysfunction could lead to abnormal electrical coupling between cells which could cause arrhythmia [20]. Cx43 participated not only in the formation of gap junctions between cells but also in the formation of L-type calcium channel molecular complexes [21], the regulation of outward potassium currents [22], and the composition of sodium channels [23]. Li et al. [24] radiated SD rats with electromagnetic pulses with a field strength of 200 kV/m, a pulse frequency



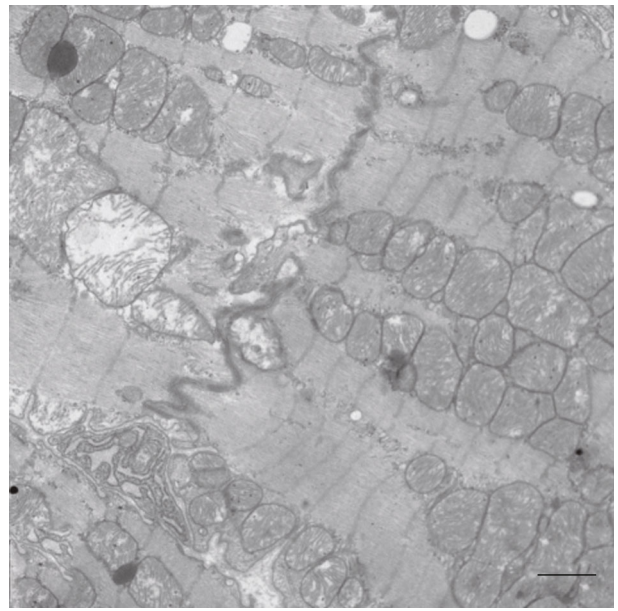
(a)



(b)



(c)



(d)

FIGURE 6: Continued.

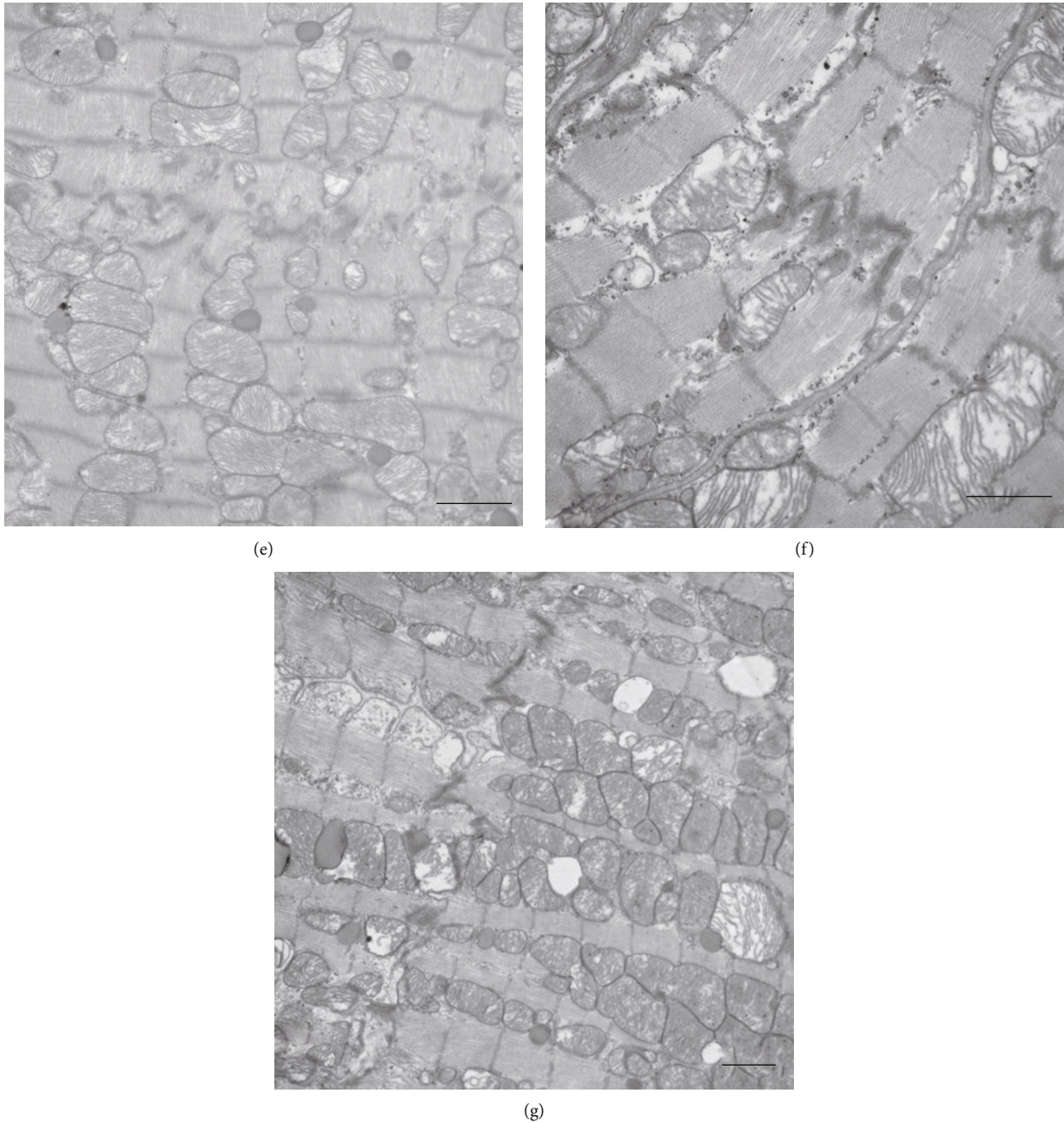


FIGURE 6: Changes of myocardial ultrastructure of rats on the 7th day after S- and X-band microwave exposure. (a) C group ($\times 15000$). (b) S5 group ($\times 10000$). (c) S10 group ($\times 20000$). (d) X5 group ($\times 12000$). (e) X10 group ($\times 12000$). (f) SX5 group ($\times 20000$). (g) SX10 group ($\times 12000$). Scale bar = $1 \mu\text{m}$.

of 200 times, and a pulse interval of 2 seconds. Based on the research, the expression of Cx43 decreased in the heart. Nav1.5 was the α subunit of the sodium channel in heart tissue and was the main channel for Na^+ flow [25]. Another study found that the reduction or absence of Cx43 expression could cause the shortening of the action potential time course, the expression of Nav1.5, and the reduction of sodium current mediated by it [26]. It was suggested that the downregulation of Cx43 and Nav1.5 increased the susceptibility of conduction disorders and arrhythmia [27].

Cx43 has also been shown to be widely present in immune cells [28, 29], which could regulate lymphocyte activation and inflammatory cytokine production [30].

The damage to the electrical conduction function of the heart after microwave radiation had been confirmed, but the damage mechanism had not been elucidated. In order to explore the mechanism of injury, this study focused on the role of Cx43 in the damage of cardiac electrical conduction after microwave composite exposure. By using immunohistochemistry, western blotting, and image analysis

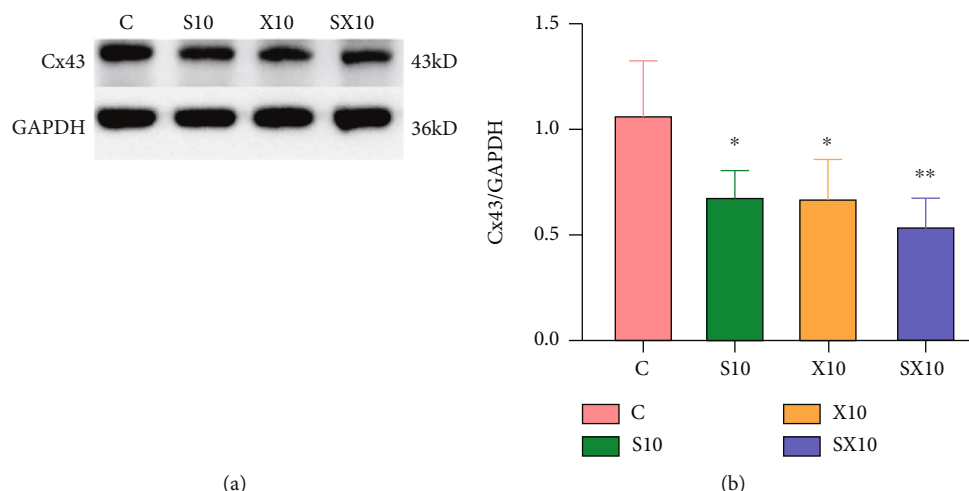


FIGURE 7: Changes of Cx43 expression in rats' myocardial tissue on the 7th day after microwave radiation. (a) Cx43 protein bands. (b) Western blot quantitative analysis results.

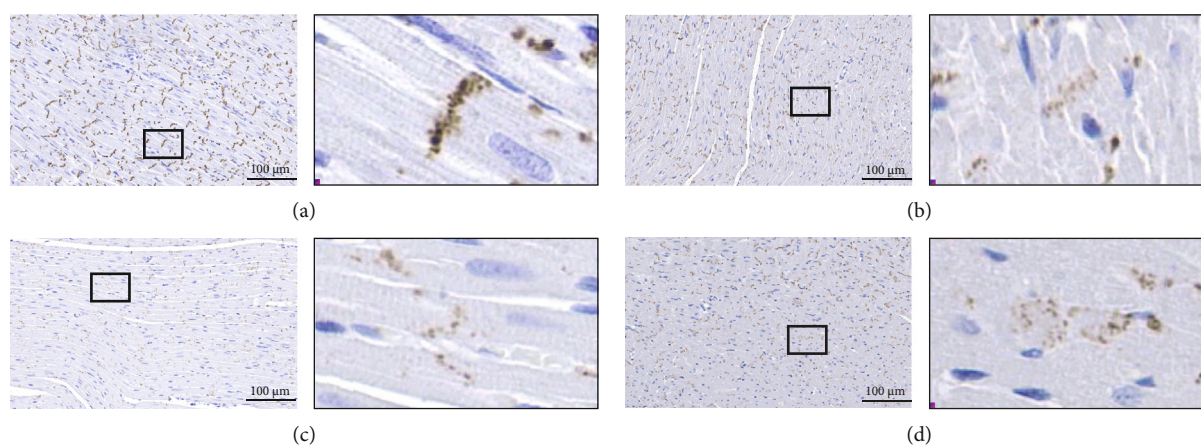


FIGURE 8: Changes of Cx43 distribution in rats' myocardial tissue on the 7th day after microwave radiation. (a) C group. (b) S10 group. (c) X10 group. (d) SX10 group. (a–d) $\times 400$. Scale bar = 100 μm .

techniques to study the changes of Cx43 in rats' myocardial tissue after microwave composite exposure. The Cx43 expression clearly decreased, and its distribution was disordered after microwave radiation of 10 mW/cm²; also, the SX10 group suffered the most serious damage. The S10 and X10 groups were severely injured, but there was no difference between the two groups. The above results suggested that the decrease of Cx43 expression and abnormal distribution might lead to abnormal electrical conduction in the heart, but how to analyze the relationship between Cx43 and abnormal electrical conduction requires further study.

This research has potential limitations. Due to the inconsistent installation conditions of the microwave radiation sources in various laboratories, there is a lack of repeatability in the radiation conditions and the method of establishing the model. In addition, due to the characteristics of microwaves, it is necessary to use nonmetallic materials while carrying out biological effect experiments, which greatly limits the collection of some real-time data. The abovementioned problems are also common problems

in this field, and there is an urgent need to introduce scientific research instruments with the function of shielding electromagnetic signals.

5. Conclusion

In conclusion, abnormal heart function and myocardial structure damage in rats after exposure suggested that the heart injury model after S- and X-band microwave radiation was successfully established. Based on this model, the research also provided a possible mechanism for the abnormal electrical conduction of the heart after exposure; that is, the decreased and abnormal distribution of Cx43 after exposure could cause damage to the electrical conduction function of the heart. This experiment provided a new direction for the exploration of the abnormal electrical conduction mechanism of the heart after microwave radiation and provided a new intervention target for the study of damage prevention methods.

Abbreviations

Cx43:	Connexin43
SPF:	Specific-pathogen-free
ECG:	Electrocardiogram
TEM:	Transmission electron microscope
AST:	Aspartate aminotransferase
CK:	Creatine kinase
LDH:	Lactate dehydrogenase
H&E:	Hematoxylin and eosin
PBS:	Phosphate-buffered saline
BCA:	Bicinchoninic acid
SDS-PAGE:	Sodium dodecyl sulfate-polyacrylamide gel electrophoresis
TBST:	Tris-buffered saline with Tween-20
GAPDH:	Glyceraldehyde 3-phosphate dehydrogenase
HRP:	Horseradish peroxidase
DAB:	Diaminobenzidine
SD:	Standard deviation
ANOVA:	Analysis of variance
BPM:	Beat per minute
SD:	Sprague Dawley
Nav1.5:	Sodium channel protein 1.5 subtype.

Data Availability

The data used to support the findings of this study are included within the article.

Conflicts of Interest

The authors declare no competing financial and nonfinancial competing interests.

Acknowledgments

We were financed in one way: the National Natural Science Foundation of China (Grant 81402629).

References

- [1] R. Varghese, A. Majumdar, G. Kumar, and A. Shukla, "Rats exposed to 2.45 GHz of non-ionizing radiation exhibit behavioral changes with increased brain expression of apoptotic caspase 3," *Pathophysiology*, vol. 25, no. 1, pp. 19–30, 2018.
- [2] P. Chauhan, H. N. Verma, R. Sisodia, and K. K. Kesari, "Microwave radiation (2.45 GHz)-induced oxidative stress: whole-body exposure effect on histopathology of Wistar rats," *Electromagnetic Biology and Medicine*, vol. 36, no. 1, pp. 20–30, 2017.
- [3] J. Kaszuba-Zwońska, J. Gremba, B. Gałdzińska-Calik, K. Wójcik-Piotrowicz, and P. J. Thor, "Electromagnetic field induced biological effects in humans," *Przegląd Lekarski*, vol. 72, no. 11, pp. 636–641, 2015.
- [4] L. Falcioni, L. Bua, E. Tibaldi et al., "Report of final results regarding brain and heart tumors in Sprague-Dawley rats exposed from prenatal life until natural death to mobile phone radiofrequency field representative of a 1.8 GHz GSM base station environmental emission," *Environmental Research*, vol. 165, pp. 496–503, 2018.
- [5] X. P. Xu, S. X. Wang, Y. Li et al., "Effects of microwave radiation on physiological functions of important organs in rhesus monkeys," *Military Medical Sciences*, vol. 35, no. 5, pp. 355–360, 2011.
- [6] J. Zhang, B. Zhang, H. Wang et al., "Quantitative studies on the biological long-term effects of heart injury in rats induced by microwave radiation," *Chinese Journal of Stereology and Image Analysis*, vol. 22, no. 1, pp. 1–9, 2017.
- [7] E. A. Adebayo, A. O. Adeeyo, M. A. Ogundiran, and O. Olabisi, "Bio-physical effects of radiofrequency electromagnetic radiation (RF-EMR) on blood parameters, spermatozoa, liver, kidney and heart of albino rats," *Journal of King Saud University – Science*, vol. 31, no. 4, pp. 813–821, 2019.
- [8] K. Boengler, S. Rohrbach, N. Weissmann, and R. Schulz, "Importance of Cx43 for right ventricular function," *International Journal of Molecular Sciences*, vol. 22, no. 3, p. 987, 2021.
- [9] K. Khosla, C. C. Naus, and W. C. Sin, "Cx43 in neural progenitors promotes glioma invasion in a 3D culture system," *International Journal of Molecular Sciences*, vol. 21, no. 15, p. 5216, 2020.
- [10] A. Tittarelli, M. Navarrete, M. A. Gleisner, P. Gebicke-Haerter, and F. Salazar-Onfray, "Connexin-mediated signaling at the immunological synapse," *International Journal of Molecular Sciences*, vol. 21, no. 10, p. 3736, 2020.
- [11] M. Chasampalioti, A. R. Green, I. O. Ellis et al., "Connexin 43 is an independent predictor of patient outcome in breast cancer patients," *Breast Cancer Research and Treatment*, vol. 174, no. 1, pp. 93–102, 2019.
- [12] A. Beckmann, M. Schubert, N. Hainz et al., "Ultrastructural demonstration of Cx43 gap junctions in induced pluripotent stem cells from human cord blood," *Histochemistry and Cell Biological*, vol. 146, no. 5, pp. 529–537, 2016.
- [13] B. Yan, Y. Q. Du, X. Y. Di, Y. S. Zou, and H. M. Zhang, "Study on abnormal QRS duration and expression of Cx43 and its phosphorylation level at Ser368 in mercury poisoning rats," *Chinese Journal of Industrial Medicine*, vol. 33, no. 5, p. 400, 2020.
- [14] X. X. Yan, Z. Zeng, M. Chen, C. Li, S. Li, and D. L. Luo, "Gap junction-associated Na⁺ influx is involved in the mediation of Ca²⁺ transients in neonatal rat ventricular myocytes," *Journal of Cardiovascular Pharmacology*, vol. 66, no. 1, pp. 41–49, 2015.
- [15] F. Ek-Vitorin, T. K. Pontifex, and J. M. Burt, "Cx43 channel gating and permeation: multiple phosphorylation-dependent roles of the carboxyl terminus," *International Journal of Molecular Sciences*, vol. 19, no. 6, p. 1659, 2018.
- [16] Y. Dou, M. F. Zhang, R. Y. Peng et al., "Effects on rat hearts induced by three kinds of band electromagnetic radiation," *Chinese Journal of Radiological Medicine and Protection*, vol. 29, no. 1, pp. 114–116, 2018.
- [17] T. Desplantez, "Cardiac Cx43, Cx40 and Cx45 co-assembling: involvement of connexins epitopes in formation of hemichannels and gap junction channels," *BMC Cell Biology*, vol. 18, no. S1, p. 3, 2017.
- [18] A. L. Drane, R. Atencia, S. M. Cooper et al., "Evaluation of relationships between results of electrocardiography and echocardiography in 341 chimpanzees (Pan troglodytes)," *American Journal of Veterinary Research*, vol. 81, no. 6, pp. 488–498, 2020.
- [19] N. E. Farag, M. K. el-Kherbetawy, H. M. Ismail et al., "Differential effect of three macrolide antibiotics on cardiac pathology

and electrophysiology in a myocardial infarction rat model: influence on sodium Nav1.5 channel expression,” *Pharmaceuticals*, vol. 14, no. 7, p. 597, 2021.

- [20] W. T. Chen, S. Y. Chen, D. W. Wu, C. C. Lee, and T. M. Lee, “Effect of icosapent ethyl on susceptibility to ventricular arrhythmias in postinfarcted rat hearts: role of GPR120-mediated connexin43 phosphorylation,” *Journal of Cellular and Molecular Medicine*, vol. 24, no. 16, pp. 9267–9279, 2020.
- [21] F. Rao, Y. M. Xue, C. Y. Deng et al., “Cx43 is involved in electrical remodeling of atrial myocytes through regulating L-type calcium current,” *Chinese Journal of Pathophysiology*, vol. 31, no. 11, pp. 1986–1991, 2015.
- [22] X. D. Li, L. Ye, Y. Zhao, N. N. Zhou, and R. Wang, “Connexin43 gene knockout mice lead to decrease of action potential duration and increase of the potassium current,” *Chinese Journal of Cardiac Pacing and Electrophysiology*, vol. 24, no. 1, pp. 60–62, 2010.
- [23] A. Leo-Macias, E. Agullo-Pascual, and M. Delmar, “The cardiac connexome: non-canonical functions of connexin43 and their role in cardiac arrhythmias,” *Seminars in Cell & Developmental Biology*, vol. 50, pp. 13–21, 2016.
- [24] X. J. Li, D. Q. Ren, Y. C. Zhou et al., “Effects of EMP on morphology of rat’s myocardial intercalated discs and the expression of Zo-1 and Cx43 proteins,” *Chinese Heart Journal*, vol. 20, no. 4, pp. 389–393, 2008.
- [25] Y. Chen-Izu, R. M. Shaw, G. S. Pitt et al., “Na⁺ channel function, regulation, structure, trafficking and sequestration,” *The Journal of Physiology*, vol. 593, no. 6, pp. 1347–1360, 2015.
- [26] M. Delmar, “Connexin43 regulates sodium current; ankyrin-G modulates gap junctions: the intercalated disc exchanger,” *Cardiovascular Research*, vol. 93, no. 2, pp. 220–222, 2012.
- [27] J. A. Jansen, M. Noorman, H. Musa et al., “Reduced heterogeneous expression of Cx43 results in decreased Nav1.5 expression and reduced sodium current that accounts for arrhythmia vulnerability in conditional Cx43 knockout mice,” *Heart Rhythm*, vol. 9, no. 4, pp. 600–607, 2012.
- [28] A. Mendoza-Naranjo, G. Bouma, C. Pereda et al., “Functional gap junctions accumulate at the immunological synapse and contribute to T cell activation,” *Journal of Immunology*, vol. 187, no. 6, pp. 3121–3132, 2011.
- [29] Y. R. Huang, Z. M. Mao, X. L. Zhang et al., “Connexin43 is required for the effective activation of spleen cells and immunoglobulin production,” *International Journal of Molecular Sciences*, vol. 20, no. 22, p. 5789, 2019.
- [30] H. C. Zhang, Z. S. Zhang, L. Zhang et al., “Connexin 43 in splenic lymphocytes is involved in the regulation of CD4⁺ CD25⁺ T lymphocyte proliferation and cytokine production in hypertensive inflammation,” *International Journal of Molecular Medicine*, vol. 41, no. 1, pp. 13–24, 2018.